

LIZARDITE AND ITS PARENT ENSTATITE: A STUDY BY X-RAY DIFFRACTION AND TRANSMISSION ELECTRON MICROSCOPY

FREDERICK J. WICKS

Department of Mineralogy and Geology, Royal Ontario Museum, 100 Queen's Park, Toronto, Ontario M5S 2C6

ABSTRACT

Transmission electron microscopy (TEM) studies on an orthopyroxene bastite have confirmed the existence of the planar structures in lizardite and a variety of variously curved serpentine structures that were observed in previous studies. The curved structures include simple curves at the end of planar structures, complete 180° curves forming hair-pin structures, tightly curved "chrysotile-like" structures and ribbon structures. Single-crystal X-ray-diffraction studies of orientation of one partly serpentinized grain of enstatite reveal a complex relationship between the parent enstatite and the replacement lizardite-1T. Forty percent of the lizardite is aligned with $X_{liz} \parallel Z_{en}$, $Y_{liz} \parallel Y_{en}$, $Z_{liz} \parallel X_{en}$, 6% is aligned with $X_{liz} \parallel Z_{en}$, $Y_{liz} \parallel X_{en}$, $Z_{liz} \parallel Y_{en}$, 6% is aligned with $Z_{liz} \angle 30^\circ X_{en}$, 3% is aligned with $Z_{liz} \angle 10^\circ Z_{en}$ and 45% is in a random orientation. Although this study applies in detail only to the grain studied, it illustrates the variations of lizardite orientation and clarifies the orientation of the lizardite structures observed in the TEM studies. Lizardite forms in one of two ways: 1) either as planar structures following the planes of close-packed oxygen atoms in the parent pyroxene, with a minimum disruption of the parent structure, or 2) as curved structures and randomly oriented serpentine that suggest an extensive reorganization of the anion framework of the parent structure. Lizardite, chrysotile and antigorite have all been observed and identified by TEM. Some complex planar structures in lizardite end in gentle curves and others in tight "chrysotile-like" rolls. At present the diffraction evidence required to identify these structures is not available.

Keywords: lizardite, chrysotile, antigorite, serpentine minerals, serpentinization, pyroxene, microbeam X-ray diffraction, single-crystal diffraction, HRTEM, orientation studies.

SOMMAIRE

Des études par microscopie électronique à transmission d'une bastite formée aux dépens d'un orthopyroxène confirment l'existence de structures planes dans la lizardite et d'une variété de structures courbes telles qu'avaient été observées dans des études antérieures. Parmi ces structures courbes, on voit des courbes simples aux extrémités de structures en plan, des courbes complètes de 180° qui forment des structures en épingle, des structures à courbure serrée qui rappellent la chrysotile, et des structures rubanées. Des études conçues pour établir les relations d'orientation d'un cristal d'enstatite partiellement serpentinisé révèlent une grande complexité entre l'enstatite parent et la lizardite-1T qui la remplace. Quarante pourcent de la lizardite

montre la relation $X_{liz} \parallel Z_{en}$, $Y_{liz} \parallel Y_{en}$, $Z_{liz} \parallel X_{en}$, 6% est aligné selon $X_{liz} \parallel Z_{en}$, $Y_{liz} \parallel X_{en}$, $Z_{liz} \parallel Y_{en}$, 6% selon $Z_{liz} \angle 30^\circ X_{en}$, 3% selon $Z_{liz} \angle 10^\circ Z_{en}$, et 45% en orientation quelconque. Quoique ces résultats s'appliquent en détail au cristal étudié seulement, ils démontrent les grandes variations dans l'orientation de la lizardite et simplifient l'interprétation des structures de la lizardite observées par microscopie électronique. La lizardite apparaît selon un des deux mécanismes suivants: 1) elle forme des structures en plan qui suivent les plans d'empilement d'atomes d'oxygène dans le pyroxène parent, avec le minimum de déformation de sa structure, ou 2) elle forme des structures courbes et à orientation aléatoire, ce qui fait penser qu'il y a eu un réorganisation majeure de la trame anionique du précurseur. On a pu observer et identifier lizardite, chrysotile et antigorite par microscopie électronique à transmission. Dans certains cas, des structures complexes en plan de lizardite aboutissent en ondulations subtiles, et dans d'autres, on trouve des rouleaux serrés qui rappellent la chrysotile. Les données par diffraction X nécessaires pour identifier ces structures ne sont toujours pas disponibles.

(Traduit par la Rédaction)

Mots-clés: lizardite, chrysotile, antigorite, minéraux du groupe de la serpentine, serpentinization, pyroxène, diffraction X avec microfaisceau, diffraction par cristal unique, microscopie électronique par transmission à haute résolution, études d'orientation.

INTRODUCTION

The orientations of serpentine formed after pyroxenes, amphiboles and various sheet silicates have been studied by microbeam X-ray camera (Wicks & Zussman 1975, Wicks & Whittaker 1977, Wicks & Plant 1979), by transmission electron microscopy (TEM) of intermediate resolution (Cressey 1977, 1979) and by high-resolution transmission electron microscopy (HRTEM) (Veblen 1980, Veblen & Buseck 1979, 1981, Spinnler 1985, Livi & Veblen, in press). Several of these studies have been carried out on the same suite of specimens, but the way in which the results relate to each other, particularly the microbeam X-ray results to the TEM results, has never been established. As the two techniques are complementary, a study that correlates results from both techniques would seem appropriate.

X-ray diffraction is used here to develop an over-

view of the crystallographic relationship between serpentine and the parent pyroxene that can be used to better assess microbeam X-ray-diffraction and TEM results. The identification of some of the serpentine minerals on the basis of the curvature displayed by the (001) fringes is shown to be difficult.

PREVIOUS STUDIES

X-ray diffraction

The first study of the serpentine minerals by microbeam (50- μm diameter) X-ray camera concentrated on their identification *in situ* in thin section (Wicks & Zussman 1975). This provided the opportunity to study directly the results of replacement of parent minerals by serpentine. In that study, the replacement of orthopyroxene by lizardite-1T and the formation of a clearly recognized pseudomorph (bastite) were investigated in detail. Later studies (Wicks & Whittaker 1977, Wicks & Plant 1979) focused on the replacement of orthopyroxene, clinopyroxene, clinoamphibole, talc, chlorite and phlogopite. Lizardite-1T was identified as the dominant mineral in 38 of the 41 samples of bastite examined. Two-layer lizardite and multilayer lizardite were found to occur infrequently. Povlen-type chrysotile was identified as the dominant mineral in only 3 specimens, and normal chrysotile was identified as a minor component with lizardite-1T in one specimen. Accessory chlorite and brucite occur as an accessory to lizardite-1T in 5 and 3 samples of bastite, respectively. Antigorite was identified as forming through the recrystallization of lizardite-1T bastite in prograde regimes, but its development eventually led to the destruction and obliteration of the bastite (Wicks & Whittaker 1977, Wicks & Plant 1979).

Although bastite is dominated by lizardite-1T, it displays a perplexing array of textural variations (Wicks & Whittaker 1977). The microbeam diffraction-patterns of Wicks & Zussman (1975) have demonstrated that the fast ray in serpentine textures indicates the position of the Z axis. The slow ray indicates the position of the X or Y axis or a combination of X and Y axis positions (Fig. 5 in Wicks & Zussman 1975). Examples of lizardite bastite with Z parallel to, and with Z perpendicular to the (110) pyroxene cleavage, were observed. Some randomly oriented lizardite is usually present and, occasionally, is dominant. Preliminary work was done to determine the relationship between the parent orthopyroxene and the replacement lizardite-1T by Wicks (1969), but this information was not included in the Wicks & Zussman (1975) study. This omission makes it difficult to relate the microbeam results to the TEM results.

Transmission electron microscopy

The first TEM and X-ray study of the ordered replacement of a pyroxene by a sheet silicate was carried out by Eggleton (1975). He found that the nontronite had formed in crystallographic continuity with the parent hedenbergite ($X_{\text{non}} \parallel Z_{\text{hed}}$, $Y_{\text{non}} \parallel Y_{\text{hed}}$), and that d_{100} of hedenbergite had become the d_{001} of nontronite.

Cressey (1977, 1979) carried out the first TEM studies of pyroxene and amphibole bastite using some of the same specimens used in the Wicks & Whittaker (1977) microbeam X-ray camera study. Some of those TEM observations, such as the slightly divergent stacks of lizardite plates in clinopyroxene and amphibole bastite, and well-formed chrysotile $2M_{c1}$ fibres lying along the (110) cleavages in a clinopyroxene bastite, confirmed the microbeam-camera results (Wicks & Zussman 1975). Other TEM observations suggest less preferred orientation of lizardite than is indicated by the microbeam-camera study. The dominant product of serpentinization of both orthopyroxene and clinopyroxene grains and exsolution lamellae appears to be a randomly oriented serpentine, generally too fine grained to identify, associated with minor, more coarsely crystalline lizardite that only occasionally displays a preferred orientation, Z_{liz} aligned roughly perpendicular to the (100) of the orthopyroxene (Cressey 1979). Semicircular sections of polygonal serpentine with $Z_{\text{serp}} \parallel X_{\text{cpx}}$ appear to be unique to the serpentinized clinopyroxene in exsolution lamellae (Figs. 12, 13a, Cressey 1979).

The first HRTEM studies of the uralitization of pyroxene and serpentinization of amphibole, with point-to-point resolution of 4 Å, were carried out by Veblen & Buseck (1979, 1981) and Veblen (1980). Spinnler (1985) carried out further studies using serpentinized pyroxene characterized in the microbeam-camera studies (Wicks & Whittaker 1977, Wicks & Plant 1979). When viewed with Z_{pyr} aligned parallel to the electron beam, Veblen & Buseck (1981) found that the sheet silicates replace the parent pyroxenes with their sheets parallel to the silicate chains of the parent. Spinnler (1985) found that the serpentine sheets are roughly parallel to the length of the silicate chains in pyroxene. These are important observations because they permit the microscopist to align a partly serpentinized grain in a position that will promote the imaging of (001) fringes of sheet silicates.

Talc, chlorite and serpentine were observed within tens of ångströms of each other, occurring in discrete domains intergrown on (001) (Veblen & Buseck 1981). In addition the three principal types of serpentine structure have all been observed: the neatly rolled cylindrical structure of chrysotile (Fig. 1, Veblen & Buseck 1979), the planar structure of

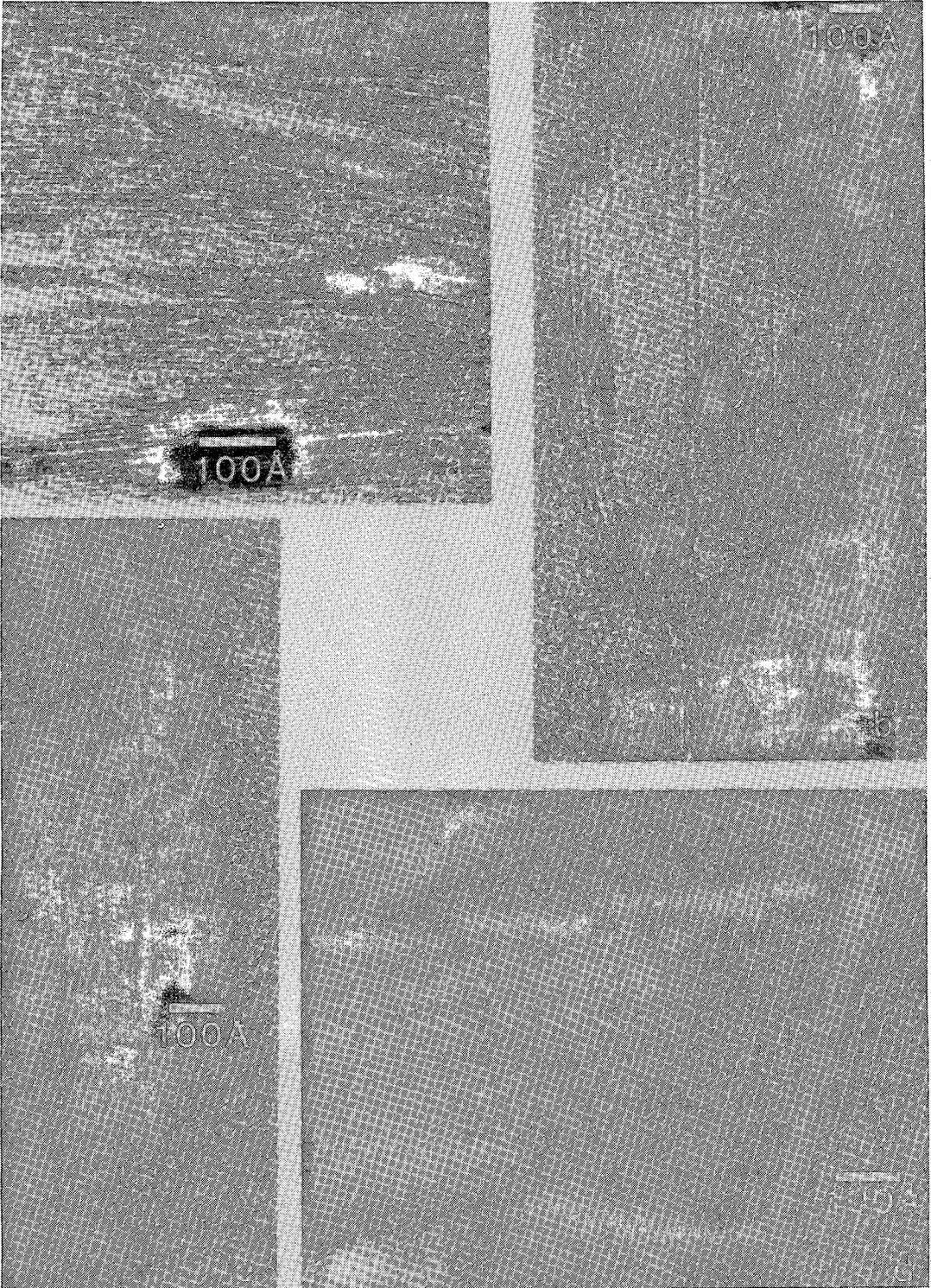


FIG. 1. Features of lizardite after enstatite. a) Subparallel alignment of lizardite grains with chlorite interlayered on (001), b) planar lizardite with chlorite interlayer on (001), c) gentle S-shaped curve in lizardite, d) a kink in lizardite, possibly a pseudomorph of a kink band in the enstatite.

lizardite (Figs. 2a, b, Veblen & Buseck 1979; Fig. 23, Veblen & Buseck 1981), and the alternating-wave structure of antigorite (Fig. 7, Veblen 1980; Fig. 7, Livi & Veblen, in press). There are also many unusual structures that do not exactly match the classic structures. Some plates of lizardite terminate in curves varying from gentle (Fig. 2a, Veblen & Buseck 1979; Fig. 23, Veblen & Buseck 1981) to tight "chrysotile-like" curls (Fig. 2b, Veblen & Buseck 1979). "Rib-bon structures" occur that are complex combinations of planar, gently curled and tightly curved structures (Fig. 25, Veblen & Buseck 1981). Malformed chrysotile structures, including S-shaped structures (Fig. 6, Veblen 1980), and corrugation-periodicity disorder and misorientation in antigorite structures, have also been noted (Fig. 8, Veblen 1980). Spinnler (1985) found, as had Cressey (1979), that randomly oriented serpentine is abundant in bastite.

The microbeam camera and the TEM studies indicate that serpentine in bastite occurs both in preferred orientation that is commonly related to the parent pyribole structure, and in random orientation. The microbeam diffraction-patterns provide an overview of the variations in orientation, and the TEM studies provide a wealth of detail of individual structures and structural variations. One of the outstanding problems of relating these studies is that neither microbeam nor TEM results have been analyzed to determine the frequency of occurrence of the various orientations and the various structures.

Correlation problems

The scale at which an observation has been made and how it relates to the scales of observation in other techniques is one more problem that has not been discussed in previous studies. In hand specimen, bastite grains between 0.5 and 1 cm are common, and the features of the parent pyribole are easily recognized. In thin section, some features of the parent pyribole such as kink bands, usually 0.4 mm (400 μm) or less in width, are preserved and recognizable even after serpentinization (Wicks 1984a). Other features, such as cleavage planes and exsolution lamellae, may be preserved or obscured depending on the exact nature of the enclosing serpentine.

The microbeam X-ray camera employs a 50- μm diameter collimator so that the diffraction pattern recorded represents the average orientation of serpentine in a cylindrical volume 50 μm in diameter and 30 μm thick. The TEM results of Cressey (1979) were published at a field of view of approximately 3 μm (30000 \AA), and no (001) fringes were resolved, whereas the results of Veblen & Buseck (1979, 1981), Veblen (1980), Spinnler (1985) and Livi & Veblen (in press) were published at a field of view of approximately 0.2 μm (2000 \AA) and (001) fringes were resolved to 4 \AA . These fields of view are 1/17 and 1/250 the diameter of the microbeam area of exposure. Obviously much larger areas were examined to obtain these (001) fringes, and the published images were chosen either to represent these larger

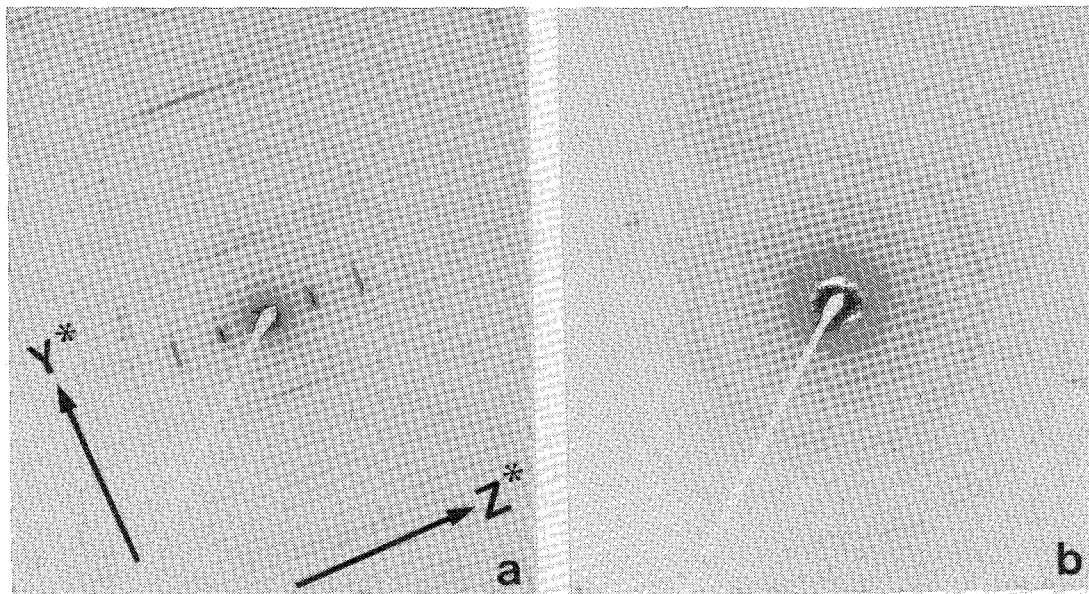


FIG. 2. a) [100] selected-area diffraction patterns of serpentine. This pattern is consistent with a lizardite-17 microbeam X-ray-diffraction pattern, but it does not uniquely identify lizardite-17; b) selected-area diffraction pattern of randomly oriented serpentine.



FIG. 3. Curved features associated with lizardite after enstatite. a) Lizardite ending in gentle curves, b) lizardite ending in a 180° "chrysotile-like" curl, c) lizardite ending in a 270° "chrysotile-like" curl, d) lizardite with an open 180° curve.

areas or to illustrate unusual structures. When one carefully examines the microbeam diffraction-patterns, the variation of serpentine orientation illustrated by the TEM micrographs is not surprising. The problem is to quantify the microbeam results to provide some orientation parameters so that significance of the more detailed TEM results can be established.

The microbeam camera used (Wicks & Zussman 1975) is limited in that the specimen is fixed in a plane perpendicular to the X-ray microbeam, making detailed studies of orientation impossible. A Unicam rotation camera with a 0.5 mm (500 μm) diameter collimator was used in the present study to overcome this problem. The specimen is exposed to an X-ray beam 10 \times broader than in the microbeam camera, but the resulting X-ray-diffraction patterns recorded from a stationary specimen are similar to the microbeam X-ray-diffraction patterns and form the basis for the present study.

STUDY BY TRANSMISSION ELECTRON MICROSCOPY

A bastite-bearing serpentinite (specimen W70-55) from the Beaver mine (C pit), Quebec, was examined on the JEOL JEM-100 CX scanning transmission electron microscope at the University of Michigan. Studies using the X-ray microbeam camera indicated that the bastite is composed of lizardite-1T and lesser chlorite intimately intergrown on (001) (Wicks & Plant 1979). A grain aligned with the former enstatite cleavage perpendicular to the plane of the thin section was selected and ion-thinned for examination by electron microscopy.

The bastite contains areas of subparallel planar 7- \AA structures (Fig. 1a) that produce [100] selected-area diffraction (SAD) patterns with arcuate reflections (Fig. 2a) consistent with the lizardite-1T microbeam diffraction-patterns (Fig. 5e, Wicks & Zussman 1975). Single or sets of two or three 14- \AA fringes are irregularly distributed, indicating chlorite layers intergrown on (001) with the lizardite (Figs. 1a, b). Some featureless areas produce randomly oriented serpentine SAD patterns (Fig. 2b). The diffuse band in the 2.6- to 2.4- \AA region in the place of sharp reflections suggests structural disorder.

Zones of well-developed 7- \AA fringes indicate that the lizardite is essentially planar (Fig. 1b), although gentle S-shaped curves are common (Figs. 1b, c). Sharp S-shaped curves also occur (Fig. 1d). The structure at the edges of planar regions may also be planar (Fig. 1b), but often curvature has developed (Fig. 3). The degree of curvature may be slight, 20-30 $^\circ$ (Fig. 3a) to great, 270 $^\circ$ and "chrysotile-like" (Fig. 3c). Overlapping planar and curved structures, the ribbon structures of Veblen & Buseck (1981), are common but not well developed (Fig. 4).

The (001) fringes were infrequently observed; thus it is clear that large areas of the bastite were not oriented with (001) parallel to the electron beam, or are composed of randomly oriented fine-grained serpentine (Fig. 2b) that does not produce (001) fringes, or are amorphous owing to ion milling or beam damage. It is difficult to assess the relative abundance of these different areas.

These results confirm the earlier studies and provide a basis for linking the TEM studies and the

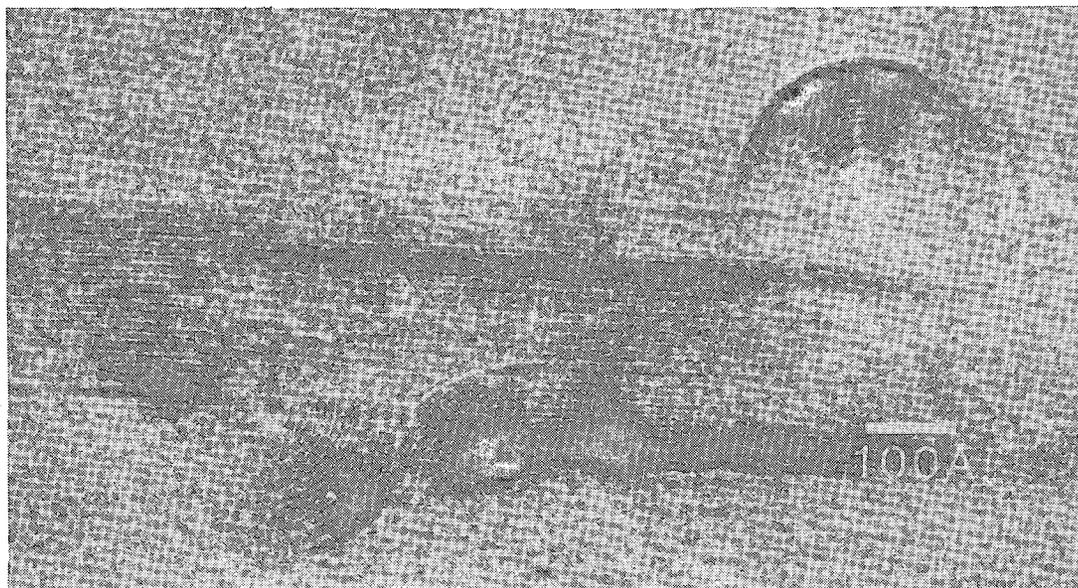


FIG. 4. Possible ribbon structure in serpentine after enstatite.

microbeam X-ray-diffraction studies. The interpretation of the X-ray-diffraction study is based on the small grain-size and subparallel alignment of the lizardite grains revealed in the TEM studies.

STUDY BY X-RAY DIFFRACTION

To establish the relationship between lizardite and the parent orthopyroxene, a partly serpentinized enstatite (En₈₇) grain was removed from a thin section of the Lizard peridotite, Cornwall (specimen 18510) and mounted in a Unicam rotation camera. This is the same sample used by Cressey (1977, 1979) and similar to one (FW-L-4) used by Spinnler (1985). The *Z* direction of the enstatite was set parallel to the rotation axis of the camera, and the *X* and *Y* were located. With the *X* direction of the enstatite parallel to the X-ray beam, the grain was translated until a lizardite-1*T* diffraction pattern was recorded (Fig. 5a). The grain was then rotated 90°, so that the *Y* direction of the enstatite was parallel to the X-ray beam, and a second lizardite-1*T* diffraction pattern recorded (Fig. 5b). Both lizardite diffraction-patterns were recorded from a stationary grain on flat films, thereby allowing direct comparison with microbeam diffraction-patterns.

Individual reflections occur as spots or short arcs superimposed on weak, but usually complete, diffraction rings (Fig. 5). The complex diffraction-patterns reveal five distinct lizardite-1*T* orientations within a cylindrical volume 0.5 mm in diameter and 0.03 mm thick. The spread of most reflections into arcs indicates a significant rotational disorder of the lizardite-1*T* grains. The interpretation of the five superimposed diffraction-patterns will be presented in order of decreasing overall intensity (abundance of sample) and decreasing complexity of the diffraction patterns. Indexing of the diffraction patterns has been carried out using a conventional, single-layer, orthohexagonal cell.

Primary orientation

The most intense diffraction-pattern is produced when the composite enstatite-lizardite grain is aligned with X_{opx} parallel to the X-ray beam. It approximates a [001] lizardite-1*T* diffraction pattern (Fig. 6a), indicating that Z_{liz} is approximately parallel to X_{opx} . The diffraction spots are slightly broadened and form a hexagonal array. A much larger number of reflections are recorded than would be expected for a stationary single crystal (Fig. 5a). For the 201 and equivalent 131 planes to be in a diffracting position, the lizardite structure need only be tilted 2° from the alignment of Z_{liz} parallel to the X-ray beam in a plane containing the X-ray beam and the normal to the diffraction spot (Table 1). The 020 and equivalent 110 reflections indicate 10° of tilt-

ing (Table 1). The 200 and 202 reflections are absent, but the equivalent 130 and 132 reflections are present and indicate 17° and 15° of tilting, respectively (Table 1). The absence of the 200 and 202 reflections indicates that the tilting of *Z* away from the X-ray beam in the *X, Z* plane is less than 15° (Table 1). These observations suggest a systematic tilting of some of the lizardite-1*T* away from the position with *Z* parallel to the X-ray beam. The TEM observations (Figs. 1, 3, 4; also, Veblen & Buseck 1981, Spinnler 1985) indicate that the area irradiated is not a single crystal but an assemblage of subparallel grains, many of which are curved to some degree. The X-ray-diffraction pattern suggests that the angular variation of the position of these subparallel grains varies continuously over a range of at least 34° ($2 \times 17^\circ$ for 130: Table 1) in the plane containing the X-ray beam and the normal to the 130 reflections, and over less than 30° ($2 \times 15^\circ$ for 202, Table 1) in the *X, Z* plane.

When the composite grain was rotated 90° so that Y_{opx} is parallel to the X-ray beam, a diffraction pattern approximating a [010] lizardite-1*T* diffraction pattern is produced. This indicates that the average position of Y_{liz} is parallel to Y_{opx} (Fig. 6b). The 00*l* reflections are spread out into arcs of 25° to 30° (measured on 002), indicating up to $\pm 15^\circ$ of tilting on *Z* in the *X, Z* plane away from the ideal position (Table 1). Very weak 003 reflections can be detected on the film, indicating tilting of at least 18° of *Z* in the *Y, Z* plane (Table 1). The 201 reflections indicate 18° of tilting (Table 1), but the 200 reflections are absent and indicate that the tilting of *X* in the *X, Y* plane is less than 17° (Table 1).

The average position of lizardite-1*T* in the primary orientation is $X_{\text{liz}} \parallel Z_{\text{en}}, Y_{\text{liz}} \parallel Y_{\text{en}}, Z_{\text{liz}} \parallel X_{\text{en}}$. However, the actual position of the individual lizardite grains varies over at least 36° in the *Y, Z* plane and 25° to 30° in the *X, Z* and *X, Y* planes.

Secondary orientation

Lizardite-1*T* in a secondary orientation is indicated by a weak [010] diffraction pattern superimposed upon the stronger, primary [001] diffraction pattern (Figs. 5a, 6c) and by a weak [001] diffraction pattern superimposed upon the primary [010] diffraction pattern (Figs. 5b, 6d). Thus the lizardite-1*T* that produces the secondary diffraction-patterns has its average *X* position aligned parallel to the average *X* of the primary lizardite-1*T*, but it is rotated 90° about the *X* axis with respect to the primary orientation. In most respects the [001] and [010] diffraction patterns of the lizardite-1*T* in the secondary orientation are similar to the primary diffraction-patterns (Fig. 6) but indicate a more strongly developed preferred orientation. The 020 reflections are 1/3 the intensity of the 110 reflections (Fig. 5b, Table 2), indicating that there is less rotation of lizardite

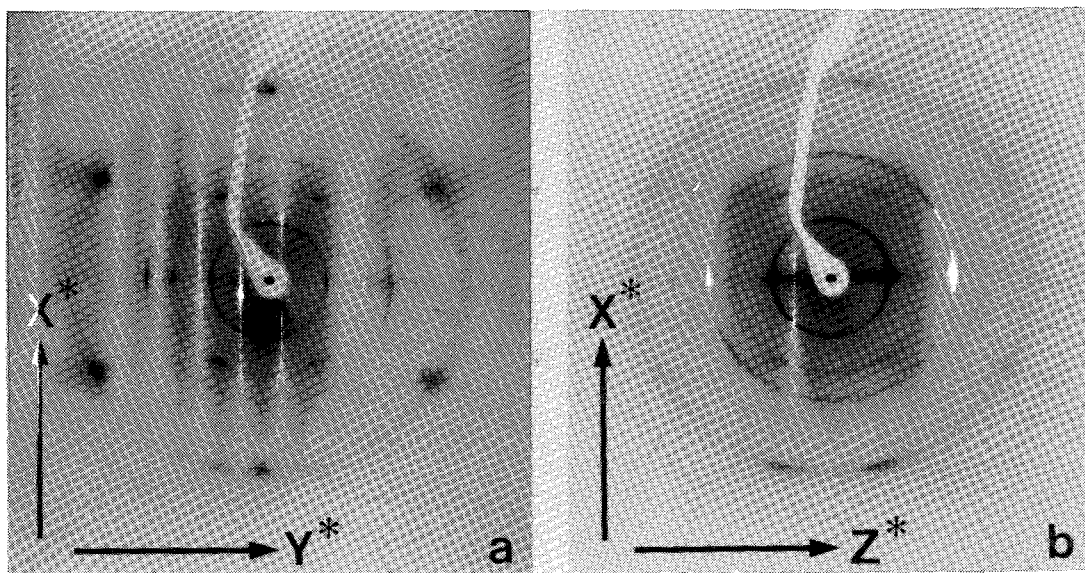


FIG. 5. X-ray-diffraction pattern of lizardite-1*T* recorded when a) Z_{en} is vertical and X_{en} is parallel to the X-ray beam, and b) when Z_{en} is vertical and Y_{en} is parallel to the X-ray beam. The axes on the patterns refer to the lizardite in the primary orientation.

grains about X in the secondary orientation. The absence of the 201 reflections suggests a strong parallelism of the lizardite grains along X . The average position of the lizardite-1*T* in secondary orientation approximates $X_{liz} \parallel Z_{en}$, $Y_{liz} \parallel X_{en}$, $Z_{liz} \parallel Y_{en}$.

Ternary and quaternary orientations

A ternary orientation of lizardite-1*T* is indicated by 00*l* reflections that are spread into 25–30° arcs located at 30° away from the main 00*l* reflections on the primary [010] diffraction pattern (Figs. 2b, 6f). No other reflections are recorded in association with these 00*l* reflections, so that the X and Y positions cannot be located. Only the relationship $Z_{liz} \angle 30^\circ Y_{en}$ can be specified for the ternary orientation.

TABLE 1. TILTING REQUIRED FOR DIFFRACTION

hkl	Type of diffraction pattern	
	[010]	[001]
200 = 130	17°	17°
201 = 131	18	2
202 = 132	21	15
020 = 110	—	10°
001	6°	—
002	12	—
003	18	—

Direction of tilting given in the text.

TABLE 2. AVERAGE INTENSITIES OF SELECTED DIFFRACTION RINGS FROM THE ROTATION CAMERA PATTERNS

Position*	Fig. 5a	Fig. 5b
	020 Ring	002 Ring
0°	3	3
15°	2	2
30°	23	2
45°	1	2
60°	2	2
75°	2	4
90°	17	20
105°	2	3
120°	1	2
135°	1	2
150°	17	1
165°	<u>1</u>	<u>3</u>
TOTAL	72	46

*The 0° position is at the top centre of the diffraction ring. Each intensity represents the average of two positions 180° apart. eg. 0° = 1 at 0° + 1 at 180°. On the 020 ring 30° = 110 reflection, 90° = 020 reflection and 150° = 110 reflections.

Similarly, a quaternary lizardite-1*T* orientation is indicated by weak 00*l* reflections also spread into 25–30° arcs aligned so that the quaternary Z direction is at an angle of 5 to 10° to Z_{en} . This is at 5 to 10° to the X position of the primary and secondary orientations (Figs. 5a, b, 6e, f). No other reflections that would indicate the position of X and Y were recorded, so that only the relationship $Z_{liz} \angle 10^\circ Z_{en}$ can be specified for the quaternary orientation.

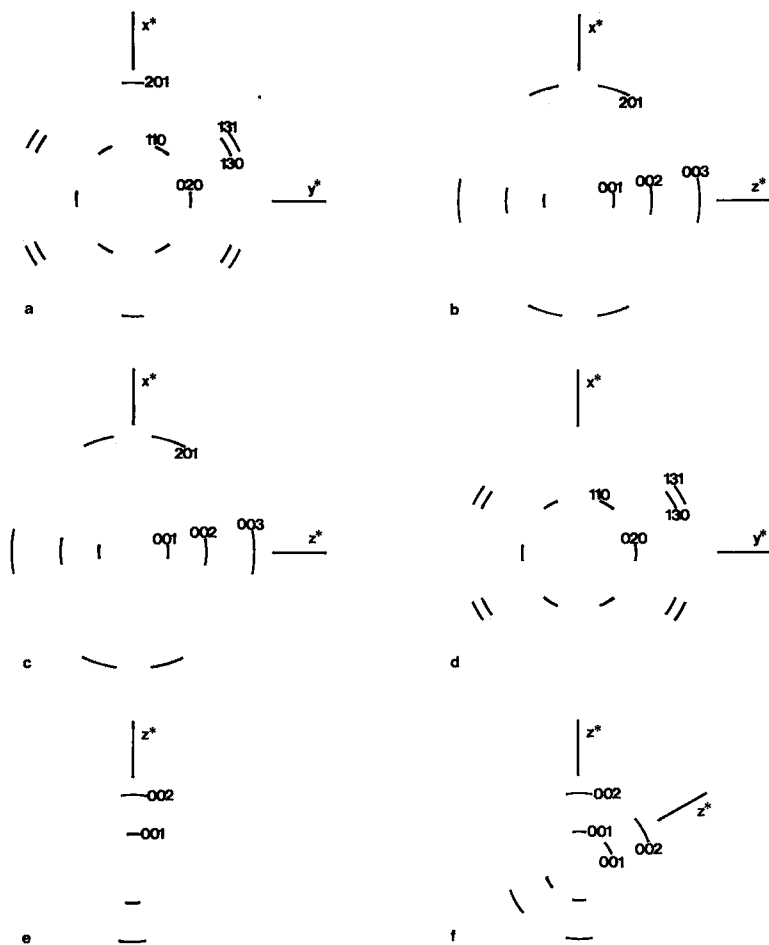


FIG. 6. The left column of the diagram (a, c and e) relates to the lizardite-1*T* X-ray-diffraction pattern in Figure 5a, and the right column (b, d and f), to the pattern in Figure 5b. a) [011] pattern, primary orientation; b) [010] pattern, primary orientation; c) [010] pattern, secondary orientation; d) [001] pattern, secondary orientation; e) 00/ reflections, quaternary orientation, and f) vertical 00/ reflections, quaternary orientation. The inclined 00/ reflections: ternary orientation.

Random orientation

In association with these four partially oriented, superimposed diffraction-patterns from four distinct orientations of lizardite, there is also the randomly oriented lizardite-1*T* that produces the weak, relatively uniform diffraction-rings (Table 2) in both of the diffraction patterns recorded (Figs. 5a, b).

Intensity distribution

Intensity measurements at 15° intervals about the 002 diffraction ring (Table 2), using an Officina Elet-

rotecnica di Tenno densitometer, indicate that the randomly oriented lizardite-1*T* is not uniformly distributed between the two diffraction patterns recorded. The 002 ring is more intense on the [010] pattern (Fig. 5a) than on the [001] pattern (Fig. 5b). Although it is difficult to estimate the amount of lizardite-1*T* in each orientation, an approximation can be made by assuming a uniform gradation between the two measured diffraction-rings at 15° intervals over the quadrant of a sphere representing the 002 surface. The distribution of the lizardite-1*T* among the five orientations obtained is: primary orientation 40%, secondary 6%, ternary 6%, quaternary 3%, and randomly oriented 45%.

DISCUSSION

It must be emphasized that the control of the parent enstatite over the lizardite-1*T* that replaces it is not rigorous. The four orientations of lizardite observed are average positions of related subparallel grains of lizardite that are rotated some 25 to 36° with respect to each other and about a particular direction in parent enstatite. The primary orientation (40%), $X_{\text{liz}} \parallel Z_{\text{en}}$, $Y_{\text{liz}} \parallel Y_{\text{en}}$, $Z_{\text{liz}} \parallel X_{\text{en}}$, and the secondary orientation (6%) $X_{\text{liz}} \parallel Z_{\text{en}}$, $Y_{\text{liz}} \parallel X_{\text{en}}$, $Z_{\text{liz}} \parallel Y_{\text{en}}$, have one feature in common. Both are oriented so that $X_{\text{liz}} \parallel Z_{\text{en}}$. This is not a universal feature, however, for in the quaternary orientation (3%) Z_{liz} is subparallel to Z_{en} . Although the relationship between the enstatite and lizardite is not precise, some of the silicate chains in the enstatite do form the foundation of some of the replacement lizardite. However, the 45% lizardite in a random orientation has not been directly influenced by the structure of the parent enstatite.

With an estimated 45% of the lizardite in random orientation, it is surprising that so many features of the original enstatite are preserved in the pseudomorph. Serpentinization does not disrupt many of the internal planar features of the enstatite, such as cleavage planes (Wicks 1984b) and boundaries of exsolution lamellae (Cressey 1979). This process, combined with the 45 to 55% of the lizardite that is structurally related to the parent enstatite, preserves many of the enstatite features.

The X-ray results obtained from this particular specimen of bastite should not be taken as representative of all samples of bastite. Even amongst different grains in this one thin section, microbeam diffraction-patterns indicate a variation in lizardite orientation relationships. Thus, although most of the microbeam diffraction-patterns recorded diffraction arcs of 30°, some recorded sharp diffraction-spots (Fig. 6k, Wicks & Zussman 1975). This indicates that within the 50- μm beam diameter, lizardite grains can be in a more strictly parallel alignment than those discussed above. This study should be taken as one example of a complex and variable system. It can, however, be used to link the previous diffraction results obtained by microbeam (Wicks & Zussman 1975) to published TEM results (Cressey 1979, Veblen 1980, Veblen & Buseck 1979, 1981, Spinnler 1985), and to the TEM results in the present study.

Application to microbeam diffraction

The oriented diffraction-patterns obtained from this composite enstatite-lizardite grain can be applied to the microbeam diffraction-patterns from other samples of bastite published earlier by Wicks & Zussman (1975) and Wicks & Whittaker (1977). The crystallographic relationship $X_{\text{liz}} \parallel Z_{\text{en}}$, $Y_{\text{liz}} \parallel Y_{\text{en}}$, $Z_{\text{liz}} \parallel X_{\text{en}}$

(the primary orientation of this study) is by far the one most commonly encountered in lizardite-1*T* bastite after enstatite (Wicks & Zussman 1975). The other orientations recorded were also found in the earlier studies, although not always within a single diffraction-pattern. Some orientations not observed in the present study were recorded in the earlier studies [e.g., Fig. 6k, and p. 252, 2nd column, 2nd paragraph, Wicks & Zussman (1975)].

As the plane of a thin section containing bastite is fixed perpendicular to the X-ray beam in the microbeam camera, there is no way to re-align a particular bastite. Thus most microbeam diffraction-patterns have been recorded from bastite oriented at some intermediate position between the two principal alignments used in the present study. As a result features of both the [010] and the [001] diffraction patterns are usually recorded (Fig. 6m, Wicks & Zussman 1975). The characteristic feature of these patterns is a marked difference in intensities between equivalent reflections across the trace of the *X* axis. This is an important diagnostic feature because these diffraction patterns have some similarities to those of chrysotile (Figs. 6a, b, Wicks & Zussman 1975), except that the cylindrical structure of chrysotile produces equal intensities across the plane containing the *X* axis. The intensity differences in the lizardite-1*T* pattern indicate that the lizardite does not have a completely random orientation about the *X* axis or have a uniformly cylindrical structure.

In some samples of orthopyroxene bastite and in many of clinopyroxene bastite, most of the lizardite occurs with Z_{liz} aligned parallel to Z_{py} . This approximates the quaternary orientation of the present study. Cressey (1979) has shown that such lizardite occurs as subparallel, slightly divergent stacks of lizardite plates (Fig. 14, Cressey 1979). Microbeam diffraction-patterns from this material have *Ok**l* reflections relating to second- and fourth-layer lines of *Y** superimposed on 2*0l* reflections relating to second-layer lines of *X** (Fig. 6g, Wicks & Zussman 1975). This superimposition of [100] and [010] diffraction patterns is produced by a variation in the alignment of the stacks of lizardite plates of over 30°. Although lizardite has been indexed on an orthohexagonal cell, it has trigonal symmetry, so every X_{ortho} chosen is only 60° away from an alternate *X* axis and only 30° away from an alternate *Y* axis. This relationship combined with a rotation of over 30° between the lizardite stacks produces the superimposed diffraction-patterns.

Application to electron microscopy

The observation of Veblen & Buseck (1981) that silicate sheets form parallel to the pyroboles chains has greatly assisted in the study of the alteration process. The orientation relationships revealed by X-ray

diffraction indicate that placing Z of an orthopyroxene parallel to an electron beam will allow the lizardite in the $X_{\text{liz}} \parallel Z_{\text{en}}$, $Y_{\text{liz}} \parallel Y_{\text{en}}$, $Z_{\text{liz}} \parallel X_{\text{en}}$ orientation (primary in this study), in the $X_{\text{liz}} \parallel Z_{\text{en}}$, $Y_{\text{liz}} \parallel X_{\text{en}}$, $Z_{\text{liz}} \parallel Y_{\text{en}}$ orientation (secondary in this study) and any found in the $X_{\text{liz}} \parallel Y_{\text{en}}$, $Y_{\text{liz}} \parallel Z_{\text{en}}$, $Z_{\text{liz}} \parallel X_{\text{en}}$ orientation (not found in this study) to be successfully imaged. This includes most of the oriented lizardite found in this study (46%), but excludes the lizardite oriented with $Z_{\text{liz}} \parallel Z_{\text{en}}$ (approximates the quaternary in this study) and that oriented with $Z_{\text{liz}} \angle 30^\circ$ to X_{en} (ternary in this study) and most of the randomly oriented lizardite. The latter at 45% is the most abundant orientation and has been encountered frequently in TEM studies (Cressey 1979, Spinnler 1985).

In order to design a HRTEM study with comprehensive coverage of all orientations of lizardite, a single-crystal X-ray-diffraction study is very useful. It provides an overview of the major orientation of the lizardite and allows the HRTEM study to be systematically planned to provide structure details of the lizardite in each orientation. In future studies on serpentinized pyroxenes, amphiboles and sheet silicates, a combination of X-ray diffraction and HRTEM studies is recommended.

Mechanisms of serpentine growth

An interpretation of these X-ray and TEM results can only be made in their proper context in the complex and varied process of serpentinization (Wicks & Whittaker 1977). Serpentinization can be divided into two types: prograde and retrograde. The main factors controlling serpentinization are temperature and the availability of water. There are other secondary factors, but they need not be discussed here.

Temperature is the most important factor in prograde serpentinization. At the highest temperatures of prograde serpentinization, all previous structures such as lizardite-bastite are obliterated, and antigorite is the only stable serpentine mineral. TEM studies of this prograde antigorite reveal well-formed antigorite structures with a uniform superlattice period and few dislocations (M. Mellini, pers. comm., July 1986). This well-crystallized material is obviously the product of a process that reached, or at least approximated, equilibrium. The antigorite found in lower-temperature prograde events, such as the antigorite + brucite assemblages in chrysotile asbestos deposits, is poorly crystalline (Wicks & Whittaker 1977, Wicks & Plant 1979). Superlattice periods are variable, and stacking disorder and structural imperfections are common (Spinnler 1985). This suggests that these are the products of a process that did not reach equilibrium. Chrysotile and lizardite commonly occur in association with this antigorite (Wicks & Whittaker 1977, Wicks & Plant

1979). Bastite is common in this assemblage, but it is mineralogically more varied than in other cases. Although lizardite is commonly the dominant mineral, mixtures of lizardite and chlorite (Figs. 1a, b) and antigorite and chlorite have been identified (Wicks & Plant 1979). Chrysotile bastite, of both normal and Povlen-type, also occurs (Wicks & Plant 1979). The development of this mineralogical diversity of curved structures, chrysotile and antigorite, and high-temperature minerals, chlorite and antigorite, is promoted by the prograde environment.

Retrograde serpentinization is characterized by lizardite and the pseudomorphism of the original minerals. It occurs over a range of low temperatures (Barnes & O'Neil 1969, Wenner & Taylor 1971); the rate of serpentinization is controlled by the progress of water into the ultramafic body (MacGregor 1962, Wolfe 1967, Martin & Fyfe 1970, MacDonald 1984). If the flow of water stops, serpentinization stops. Often, serpentinization is incomplete, and equilibrium has not been reached, as in the case of the enstatite and lizardite grain used for the X-ray-diffraction study. The pseudomorphism characteristic of this type of serpentinization is promoted by this low-energy environment, where less reorganization of material is possible.

Three types of serpentine have been observed in bastite in the various TEM studies: serpentine structurally aligned with the parent structure, curved serpentine not aligned with the parent structure, and randomly oriented serpentine. The lizardite that has developed in parallel or subparallel growth with the parent pyrobole (Figs. 1a, b, c), such as in the $X_{\text{liz}} \parallel Z_{\text{en}}$, $Y_{\text{liz}} \parallel Y_{\text{en}}$, $Z_{\text{liz}} \parallel X_{\text{en}}$ primary orientation in the present study, has done so parallel to equivalent structural elements, principally the plane of close-packed oxygen atoms in the pyroxene, and along some of the silicate chains. Most of the bonds in the pyrobole are broken during the formation of serpentine, but the fewest number will be broken by this type of lizardite growth. The second form of growth, the curved structures (Figs. 3, 4) and the third form, the randomly oriented serpentine, bear little relationship to the parent pyrobole, which suggests complete dissolution of the parent and crystallization of the reactant. The bastite specimen from the Lizard, Cornwall, used in the X-ray study and in the TEM studies of Cressey (1979) and Spinnler (1985), was produced by a retrograde serpentinization. It is only partly serpentinized. Thus the temperature of serpentinization was low, and the water supply was limited to less than that required for complete serpentinization. Perhaps in this situation the types of growth are controlled by the availability of water arriving at the reaction site. This has been noted for smectite-to-illite reactions (Yau *et al.*, in press). A limited supply of water may promote parallel growth with the minimum disruption of bonds. A plentiful

supply of water may promote the extensive dissolution of the parent and crystallization of a curved serpentine.

CRITERIA FOR IDENTIFICATION

The identification of the serpentine minerals in this paper has been based on X-ray-diffraction data from powder, rotation and microbeam cameras, and SAD techniques. The X-ray-diffraction criteria for identification of the serpentine minerals were established by Whittaker & Zussman (1956) and remain essentially unchanged, although added to by subsequent work (see the review by Wicks 1979). The serpentine minerals are divided into three basic structures: lizardite with a planar structure, chrysotile with a cylindrical structure, and antigorite with an alternating-wave structure. It must be remembered that these are ideal structures. Thus although lizardite specimens with planar structures suitable for single-crystal structure refinements have recently been discovered (Mellini 1982, Mellini & Zanazzi 1986), the lizardite crystals from the type locality, the Lizard, Cornwall, are macroscopically bent into spherical caps with an estimated 12° of bending over a 0.3 mm diameter.

Each diffraction technique has its own assets and limitations. X-ray powder diffraction is a rapid method for identifying the three basic structures and the stacking variations, the polytypes (Bailey 1969, Wicks & Whittaker 1975), within each structure type. It does not reveal any information about the morphology of the material. Chrysotile asbestos fibres and massive green vein chrysotile can give an identical pattern. Recent X-ray-diffraction studies (Middleton & Whittaker 1976) and TEM studies (Cressy & Zussman 1976, Mellini 1986) indicate that some of the massive vein material appears to be composed of cylindrical chrysotile $2M_{cl}$ cores with a polygonal overgrowth of planar chrysotile $2M_{cl}$ structure. This material is not well understood and needs further study, but it serves as an example of the limits of X-ray powder diffraction. A classic cylindrically rolled chrysotile structure and a flat sheet with a chrysotile structure cannot be distinguished by X-ray powder diffraction.

The microbeam camera has an advantage over the powder technique: it provides information on the orientation of grains and records the diffraction effects from the cylindrical chrysotile structure. Thus it can be used to distinguish between cylindrical structures and polygonal overgrowths. The rotation camera, particularly as used in this study, produces the same information (Middleton & Whittaker 1976). However, the diffraction effects recorded with the microbeam camera cannot easily be used to distinguish between a spherically bent lizardite crystal, like the type material, and a group of smaller grains in

a subparallel alignment, nor does it provide information on the numerous small curved structures observed by TEM.

As the microbeam X-ray-diffraction camera has been used frequently in studies of serpentine textures, including bastite, and as this material is commonly used in TEM studies, it is useful to assess the microbeam method further. Using measurements on a microbeam diffraction-pattern containing diffraction maxima from both lizardite and parent enstatite (specimen 18549, Mt. Albert, Que.) and the Scherrer formula for particle-size broadening given in West (1984), a particle size of the lizardite between 140 and 70 Å was calculated. These grain sizes agree reasonably with the grain sizes recorded in the present TEM study (Figs. 1, 3, 4) and in other studies (Veblen & Buseck 1979, 1981, Spinnler 1985). The calculations also suggest that chrysotile, which commonly has fibre diameters of 200 to 350 Å and wall thicknesses of 75 to 150 Å (Yada 1967, 1971), should produce sharp diffraction-patterns by the microbeam technique. Minor amounts of chrysotile, even isolated fibres distributed through a bastite, can be detected if they are in parallel alignment because equivalent diffraction-maxima from all fibres will coincide at the same point on a film to produce a detectable fibre-pattern (Wicks & Whittaker 1977, Wicks & Plant 1979). Minor amounts of randomly oriented chrysotile cannot be detected because the intensity is spread out over the entire diffraction-ring. The degree of crystallinity also affects the diffraction pattern. In some patterns diffuse fogging in the 2.6 to 2.4 Å region of the microbeam patterns suggests the presence of disordered material (Wicks & Zussman 1975), but there is no way of estimating its abundance.

SAD patterns provide information for identification, although patterns from more than one orientation may be required (Fig. 2a). These patterns are, to a first approximation, similar to those from the microbeam camera, although from a much smaller area. Similarly, very fine-grained, poorly crystallized serpentine gives diffuse diffraction-effects in the 2.6 to 2.4 Å region of the pattern (Fig. 2b).

The (001) fringes of serpentine minerals produced in TEM studies provide the only direct view of the structures we are dealing with. The three basic serpentine structures lizardite, chrysotile and antigorite have all been observed and identified (Veblen 1980, Veblen & Buseck 1979, 1981, Spinnler 1985, Livi & Veblen, in press). Commonly, SAD is possible to confirm the visual identification. However, there is a surprising variation in fine structural features and combinations of structural features, such as a planar lizardite passing into a "chrysotile-like" curl (Fig. 3b; Veblen 1980, Veblen & Buseck 1979, 1981, Spinnler 1985, Livi & Veblen, in press). SAD patterns usually cannot be obtained from these fine-

scale, isolated structures, so that diffraction data are not available to aid in the identification. The most commonly used tool is the comparison of the observed structure with the structure of a well-characterized specimen. Thus the work of Yada (1967, 1971) on chrysotile asbestos fibres provides the basis for the identification of spirally and concentrically rolled cylindrical structures of chrysotile, as well as the common growth-defects of chrysotile asbestos. Many of these features, plus others not observed by Yada, have been observed in chrysotile in bastite (Fig. 6, Veblen 1980; Fig. 1, Veblen & Buseck 1979). Similarly Yada's (1979) work on imaging the superlattice structure of antigorite and Spinnler's (1985) computer-simulated imaging of the structure provide criteria for identifying antigorite when it is aligned with X perpendicular to the electron beam (Fig. 7, Veblen 1980). Small areas of lizardite can be recognized by their planar (001) fringes and their similarity to larger areas of lizardite (001) fringes from which SAD patterns have been recorded.

Important unanswered questions remain. Approximately 50% of the lizardite in the bastite studied was related to the parent enstatite structure. Is the structure in Figure 1d a curved serpentine structure, or is it a lizardite pseudomorph of a microkink band in the parent enstatite similar to those observed with the petrographic microscope (Wicks 1984a)? How much curvature can the lizardite structure accommodate? The work of Mellini (1982) and Mellini & Zanazzi (1986) indicates that well-formed, planar lizardite crystals exist, but Rucklidge & Zussman (1965) have noted that the type lizardite is macroscopically bent into spherical caps, demonstrating curvature on a large scale. Veblen & Buseck (1981) stated that the accurate (00 l) diffraction maxima in their electron-diffraction patterns indicate a rotational disorder of the serpentine about the Z direction of the parent amphibole. The microbeam-camera data (Wicks & Zussman 1975) and the rotation-camera data in the present study also suggest rotational disorder, but in all cases this could be interpreted as curvature of a large crystal or as rotation between adjacent subparallel grains. The structure refinements (Mellini 1982, Mellini & Zanazzi 1986) and the DLS modelling (Bish 1981, Wicks & Hawthorne 1986) of the lizardite structure have demonstrated that the octahedral and tetrahedral sheets of lizardite can be linked together in a planar structure without the extreme buckling of the plane of the Mg atoms once thought to occur (Wicks & Whittaker 1975). However, the misfit between the octahedral and tetrahedral sheets will still produce an internal strain, and the structure may well curve, if it can, to relieve this misfit.

It would appear reasonable that the gentle S-shaped curve in Figure 1c would be accepted by the

lizardite structure. At the other extreme, the "chrysotile-like" rolls in Figures 3b, c and 4 certainly look like chrysotile, but there are, as yet, no diffraction data to confirm this. Chrysotile is not simply a rolled-up lizardite structure. The structures of chrysotile and lizardite are different, as has been discussed in detail by Wicks & Whittaker (1975). There is some evidence, although not conclusive, that the chrysotile structure can form the planar layers in the polygonal overgrowths of cylindrical chrysotile (Middleton & Whittaker 1976). Perhaps it is impossible for the lizardite structure to adopt such a tight curve as those in Figures 3b, c and 4, and the chrysotile structure is automatically adopted. If this is the case, how much curvature can lizardite accept? Is the broad 180° curve in Figure 3d over or under the limit?

One other consideration is that the (001) fringes only give us information in two dimensions, and we do not really know the form or continuity of a structure in the third dimension. Veblen & Buseck (1981) have been able to calculate a ribbon width of 500 Å for ribbon structures (Fig. 4), but this is a special case, and information in the third dimension is not normally available. Could the image in Figure 3a be a section through a slightly flattened spherical cap, a microscopic version of the macroscopic spherical caps found by Rucklidge & Zussman (1965)? Or is it that of a lizardite grain that ends in a curl about a single axis at each end of the grain, or are the curved ends chrysotile?

The questions of curvature posed here can be argued about but not solved at this time. We must await the microdiffraction evidence to resolve this problem. Until that time some caution should be exercised in the use of mineral names on some of these unusual curved structures.

ACKNOWLEDGEMENTS

I thank Robert A. Ramik and Errol G. Katayama of the Royal Ontario Museum for the measurement of the intensities. Discussions with Professor D. R. Peacor at the University of Michigan were very helpful, and his arrangements for access to the electron-microscope facility at Ann Arbor are appreciated. The time and effort of Drs. J. H. Lee and J. H. Ahn of the University of Michigan, in connection with the operation of the electron microscope, are gratefully acknowledged. Mary Anne Chalmers's work with the word processor is greatly appreciated. I thank Dr. G. E. Spinnler for sending me a copy of his Ph.D. thesis and Professor D. R. Veblen for a preprint of his paper on "eastonite". My thanks to the official referees, Professors S. Guggenheim and D. R. Veblen, and to an unofficial referee, Professor D. R. Peacor, for their many helpful suggestions and hearty debates on various aspects of the paper.

It is a pleasure to acknowledge the support of this project by the Natural Sciences and Engineering Research Council of Canada through an operating grant to F. J. Wicks and by the National Science Foundation through grants EAR-8313236 and EAR-8604170 to D. R. Peacor.

REFERENCES

- BAILEY, S.W. (1969): Polytypism of trioctahedral 1:1 layer silicates. *Clays Clay Minerals* **17**, 355-371.
- BARNES, I. & O'NEIL, J.R. (1969): The relationship between fluids in some fresh alpine-type ultramafics and possible modern serpentinization, western United States. *Geol. Soc. Amer. Bull.* **80**, 1947-1960.
- BISH, D.L. (1981): Distortions in the lizardite structure: a distance least-squares study. *Amer. Geophys. Union Trans.* **62**, 417 (abstr.).
- CRESSEY, B.A. (1977): *Electron Microscopic Studies of Serpentinities*. Ph.D. thesis, Univ. Manchester, Manchester, England.
- _____ (1979): Electron microscope studies of serpentine textures. *Can. Mineral.* **17**, 741-756.
- _____ & ZUSSMAN, J. (1976): Electron microscopic studies of serpentinites. *Can. Mineral.* **14**, 307-313.
- EGGLETON, R.A. (1975): Nontronite topotaxial after hedenbergite. *Amer. Mineral.* **60**, 1063-1068.
- LIVI, K.J.T. & VEBLEN, D.R. (1987): "Eastonite" from Easton, Pennsylvania: a mixture of phlogopite and a new form of serpentine. *Amer. Mineral.* **72** (in press).
- MACDONALD, A.H. (1984): *Water Diffusion Rates through Serpentinized Peridotites: Implications for Reaction Induced Dynamic and Chemical Effects in Ultramafic Rocks*. Ph.D. thesis, Univ. Western Ontario, London, Ontario.
- MACGREGOR, I.D. (1962): *Geology, Petrology and Geochemistry of the Mount Albert and Associated Ultramafic Bodies of Central Gaspé, Quebec*. M.Sc. thesis, Queen's Univ., Kingston, Ontario.
- MARTIN, B. & FYFE, W.S. (1970): Some experimental and theoretical observations on the kinetics of hydration reactions with particular reference to serpentinization. *Chem. Geol.* **6**, 185-202.
- MELLINI, M. (1982): The crystal structure of lizardite 1T: hydrogen bonds and polytypism. *Amer. Mineral.* **67**, 587-598.
- _____ (1986): Chrysotile and polygonal serpentine from the Balangero serpentinite. *Mineral. Mag.* **50**, 301-306.
- _____ & ZANAZZI, P.F. (1986): The T-O layer of lizardite: new structure refinements. *Int. Mineral. Assoc., 14th Gen. Meet., Abstr. Program*, 170.
- MIDDLETON, A.P. & WHITTAKER, E.J.W. (1976): The structure of Povlen-type chrysotile. *Can. Mineral.* **14**, 301-306.
- RUCKLIDGE, J.C. & ZUSSMAN, J. (1965): The crystal structure of the serpentine mineral, lizardite $Mg_3Si_2O_5(OH)_4$. *Acta Cryst.* **19**, 381-389.
- SPINNLER, G.E. (1985): *HRTEM Study of Antigorite, Pyroxene-Serpentine Reactions and Chlorite*. Ph.D. thesis, Arizona State Univ., Tempe, Arizona.
- VEBLEN, D.R. (1980): Anthophyllite asbestos: microstructures, intergrown sheet silicates, and mechanisms of fiber formation. *Amer. Mineral.* **65**, 1075-1086.
- _____ & BUSECK, P.R. (1979): Serpentine minerals: intergrowths and new combination structures. *Science* **206**, 1398-1400.
- _____ & _____ (1981): Hydrous pyriboles and sheet silicates in pyroxenes and uraalites: intergrowth microstructures and reaction mechanisms. *Amer. Mineral.* **66**, 1107-1134.
- WENNER, D.B. & TAYLOR, H.P., JR. (1971): Temperatures of serpentinization of ultramafic rocks based on O^{18}/O^{16} fractionation between coexisting serpentine and magnetite. *Contr. Mineral. Petrology* **32**, 165-185.
- WEST, A.R. (1984): *Solid State Chemistry and its Applications*. John Wiley & Sons, New York.
- WHITTAKER, E.J.W. & ZUSSMAN, J. (1956): The characterization of serpentine minerals by X-ray diffraction. *Mineral. Mag.* **31**, 107-126.
- WICKS, F.J. (1969): *X-ray and Optical Studies on Serpentine Minerals*. D.Phil. thesis, Oxford Univ., Oxford, England.
- _____ (1979): Mineralogy, chemistry and crystallography of chrysotile asbestos. In *Mineralogical Techniques of Asbestos Determination* (R.L. Ledoux, ed.). *Mineral. Assoc. Can., Short Course Handbook* **4**, 35-78.
- _____ (1984a): Deformation histories as recorded by serpentinites. I. Deformation prior to serpentinization. *Can. Mineral.* **22**, 185-195.
- _____ (1984b): Deformation histories as recorded by serpentinites. III. Fracture patterns developed prior to serpentinization. *Can. Mineral.* **22**, 205-209.
- _____ & HAWTHORNE, F.C. (1986): Distance least-squares modelling of the lizardite 1T structure. *Geol. Assoc. Can.-Mineral. Assoc. Can., Program Abstr.* **11**, 144.

- _____ & PLANT, A.C. (1979): Electron-microprobe and X-ray-microbeam studies of serpentine minerals. *Can. Mineral.* **17**, 785-830.
- _____ & WHITTAKER, E.J.W. (1975): A reappraisal of the structures of the serpentine minerals. *Can. Mineral.* **13**, 227-243.
- _____ & _____ (1977): Serpentine textures and serpentization. *Can. Mineral.* **15**, 459-488.
- _____ & ZUSSMAN, J. (1975): Microbeam X-ray diffraction patterns of the serpentine minerals. *Can. Mineral.* **13**, 244-258.
- WOLFE, W.J. (1967): *Petrology, Mineralogy and Geochemistry of the Blue River Ultramafic Intrusion, Cassiar District, British Columbia*. Ph.D. thesis, Yale Univ., New Haven, Connecticut.
- YADA, K. (1967): Study of chrysotile asbestos by a high resolution electron microscope. *Acta Cryst.* **23**, 704-707.
- _____ (1971): Study of microstructure of chrysotile asbestos by high resolution electron microscopy. *Acta Cryst.* **A27**, 659-664.
- _____ (1979): Microstructures of chrysotile and antigorite by high-resolution electron microscopy. *Can. Mineral.* **17**, 679-691.
- YAU, Y.C., PEACOR, D.R. & MCDOWELL, S.D. (in press): Smectite-to-illite reactions in Salton sea shales: transmission and analytical electron microscopy study. *J. Sed. Petrology*.

Received June 25, 1986, revised manuscript accepted November 11, 1986.